White paper

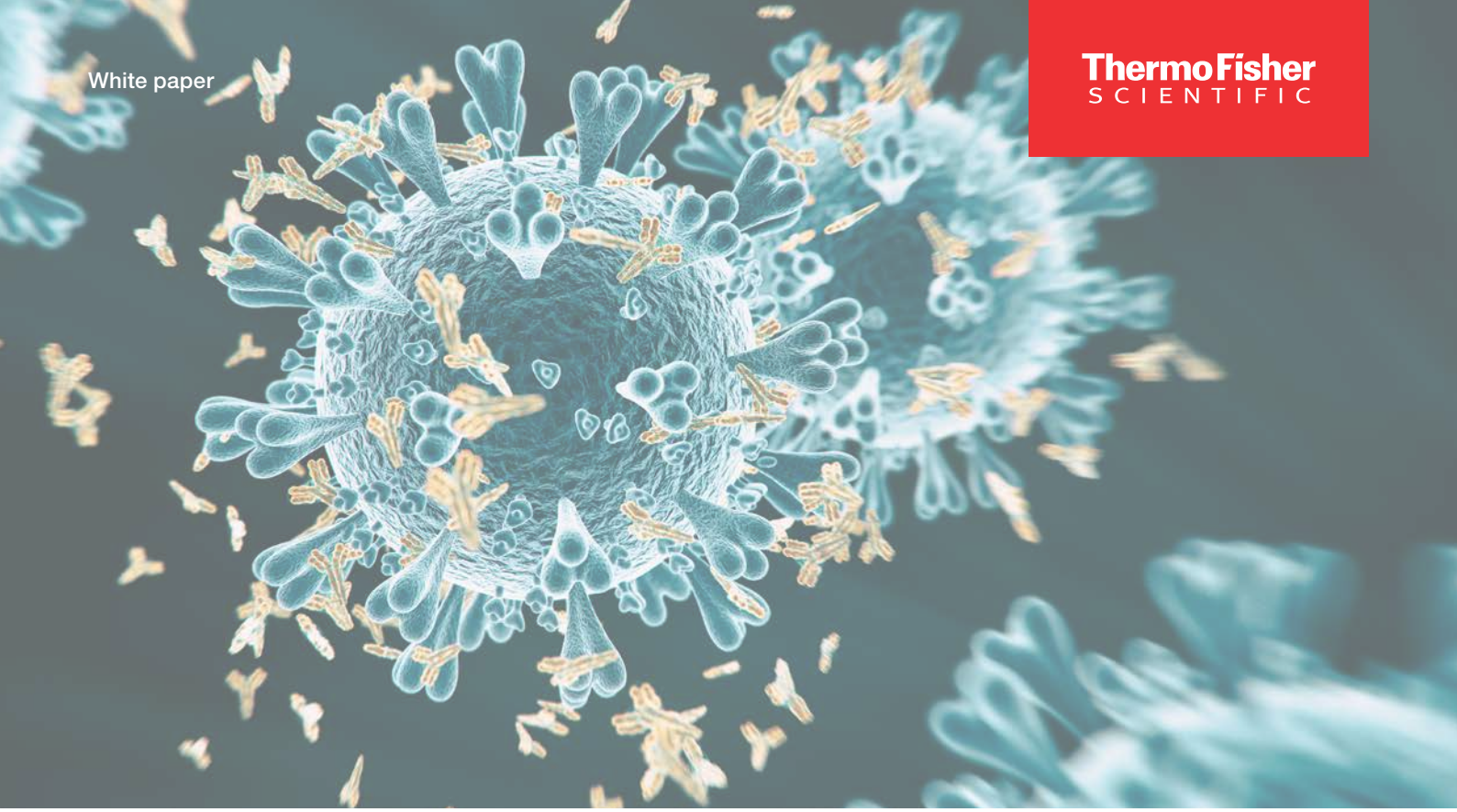

High-throughput cryo-EM epitope mapping of SARS-CoV-2 spike protein antibodies using EPU Multigrid

Authors

Ieva Drulyte[1], Stefan Koester[2], Dianna Lundberg[2], Kurt Eng[2], Andrey Malyutin[3], Aaron McGrath[3], Chunyan Wang[4], Frank van Kuppeveld[4], Berend-Jan Bosch[4], Mazdak Radjainia[1], Jerry Thomas[3], Maureen Magnay[2] and Daniel Hurdiss[4].

[1]Materials and Structural Analysis Division, Thermo Fisher Scientific, Netherlands; [2]Takeda Pharmaceuticals, Cambridge MA, USA; [3]Takeda Pharmaceuticals, San Diego, CA, USA; [4]Department of Biomolecular Health Sciences, Utrecht University, Netherlands.

Keywords

Cryo-EM, Epitope mapping, throughput, EPU Multigrid, SARS-CoV-2 Biologics, Coronavirus, COVID-19, spike protein, high-resolution, glycoprotein, drug discovery, structural biology

Introduction

Therapeutic antibodies targeting the SARS-CoV-2 spike protein can play an important role in reducing the burden of the COVID-19 pandemic by protecting vulnerable populations against severe and potentially life-threatening disease. Cryo-electron microscopy (cryo-EM) is a powerful tool for epitope mapping of antibodies that block SARS-CoV-2 virus entry [1]. Defining the epitopes of neutralizing antibodies allows us to understand their mechanism of action and to increase our knowledge of how antibodies can confer protective immunity against SARS-CoV-2. Furthermore, precise knowledge of an antibody's epitope and mechanism of action may also guide the generation of improved antibody therapeutics. For instance, cryo-EM contributed to the creation of an antibody cocktail by revealing non-overlapping epitopes to reduce the risks of viral escape [2].

One of the main concerns in the ongoing COVID-19 pandemic is SARS-CoV-2 variants that may be able to evade immunity. One such variant is the heavily mutated "Omicron" B.1.1529 strain which contains an unprecedented number of mutations in the receptor-binding domain (RBD). Epitope mapping of large antibody panels allows researchers to identify vulnerable sites on the spike protein, predict and interpret the effect of new mutations, and speed up decision-making in selecting antibody combinations that target non-overlapping epitopes. Moreover, structural information about epitopes can help identify liabilities in drug discovery pipelines in response to new emerging variants. Therefore, we asked whether cryo-EM permits rapid epitope mapping for a large antibody panel.

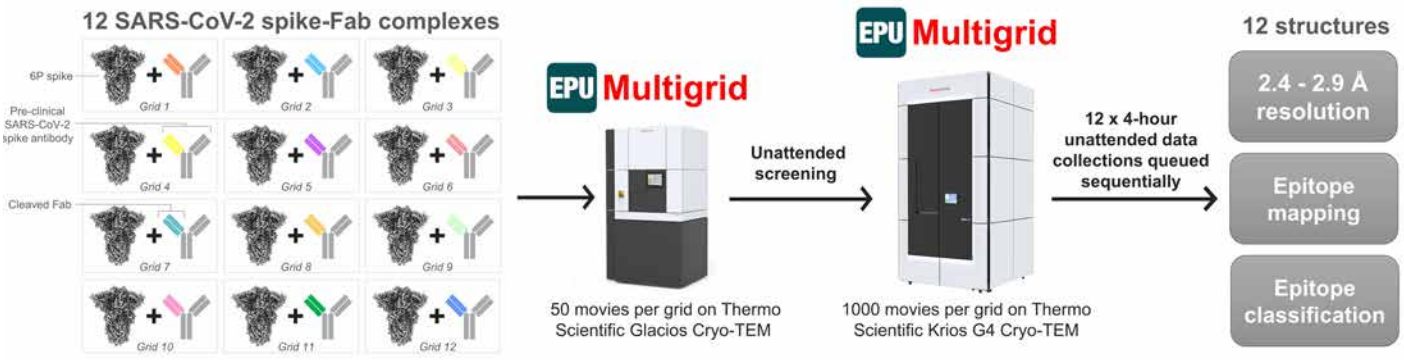

Figure 1. High-throughput cryo-EM epitope mapping of SARS-CoV-2 Spike Protein antibodies using EPU Multigrid. Spike-Fab complex grids were vitrified in duplicate and screened using Glacios cryo-TEM. Twelve best grids (one grid per complex) were taken forward for automated acquisition using Krios G4 cryo-TEM and EPU Multigrid. 48-hour EPU Multigrid session resulted in twelve sub 3 Å cryo-EM reconstructions which allowed for mapping of epitope-paratope residues, as well as assignment of Fabs to the epitope classes established in[1].

In this whitepaper, we explore how cryo-EM can be used for high-throughput epitope mapping through the multigrid data-collection capability of Thermo Scientific™ EPU Software (EPU Multigrid). A panel of neutralizing SARS-CoV-2 antibodies specific to the RBD domain was generated and characterized, with 12 pre-clinical-stage antibodies being selected for this study. This set of antibodies represents a range of SARS-CoV-2 neutralization potencies, affinities, and six differing crude epitope bins, with the majority derived from COVID-19 patients and the rest from immunizations of transgenic human IgG animals. We show how 12 sub-3-angstrom reconstructions of spike protein in complex with 12 distinct Fabs can be obtained from a 2-day unattended microscopy session (Figure 1).

EPU Multigrid for the collection of SARS-CoV-2 spike-Fab complex datasets

EPU Multigrid is a data acquisition mode for Thermo Scientific autoloader-equipped cryogenic transmission electron microscopes (cryo-TEMs) that allows users to queue multiple grids for unattended screening and data collection. In other words, up to 12 grids can be imaged in one microscope session. However, robust grid preparation and screening are critical if structures from every grid are desired. Successful grid preparation is intimately linked to protein quality and concentration. Therefore, we first established a good source of SARS-CoV-2 spike protein and vitrification conditions that reliably yield high-quality grids. We used the 6P-stabilized[3] SARS-CoV-2 pre-fusion spike ectodomain that is highly stable and amenable to dense, uniform particle distributions. To evaluate the robustness of the spike protein, we performed 1.5-hour data collection (265 movies at 175 movies/hour) using a Thermo Scientific Glacios™ Cryo-TEM equipped with a Thermo Scientific Falcon™ 4 Direct Electron Detector. Data processing yielded a 3.1 Å map of SARS-CoV-2 spike protein from 28,162 particles (Figure 2), showing that routine structure determination is possible using this spike construct.

Next, we created complexes of 6P-stabilized spike protein bound by twelve distinct Fabs (Figure 1). For grid preparation, 28 µM spike protein (based on the molecular weight of the protomer) was mixed with ~150 µM Fab fragment at a 1 to 1.4 molar ratio and incubated for 10 minutes at room temperature. Prior to plunge freezing, 0.01% (w/v) fluorinated octyl maltoside (FOM) was added to the sample to overcome the preferred orientation. The spike-Fab sample was applied to glow-

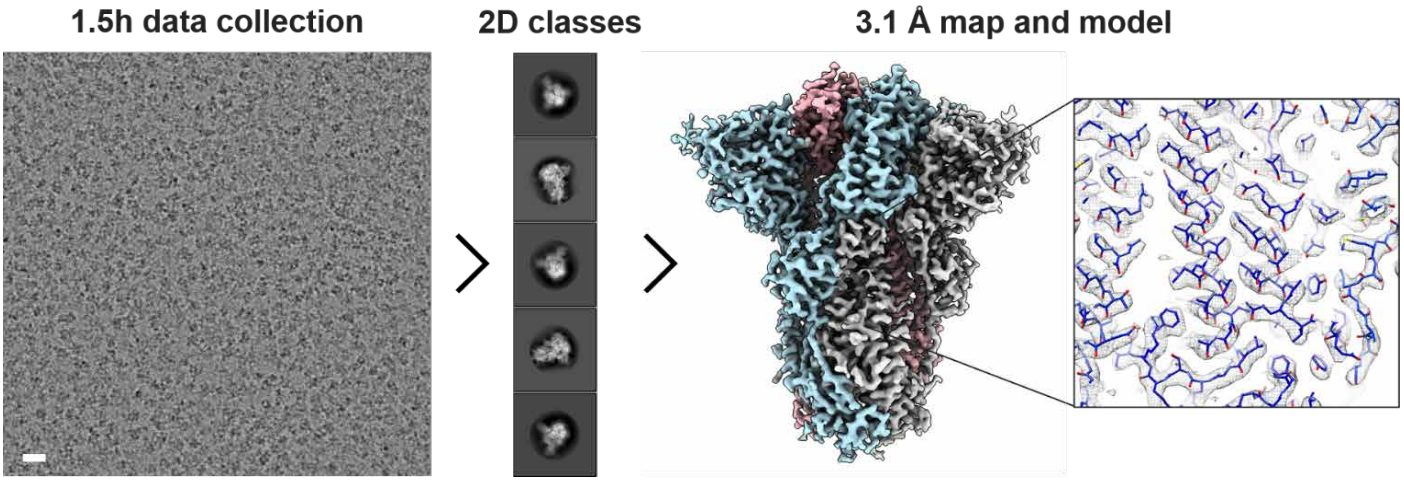

Figure 2. Single particle analysis of SARS-CoV-2 spike protein using the Glacios Cryo-TEM and Falcon 4 Detector. The Cryo-EM workflow was optimized to readily yield high-resolution SARS-CoV-2 spike structures from short data collection times. In this example, data from a 1.5 hr data collection produced a 3.1 Å spike ectodomain reconstruction from 28,162 particles. Right: Representative density containing the fitted atomic coordinates (PDB ID: 6XR8)[4]. Scale bar = 20 nm.

discharged (20 mAmp, 30 sec, Quorum GloQube) Quantifoil R1.2/1.3 grids, blotted for 5 s using blot force 0, and plunge frozen into liquid ethane using the semi-automated Thermo Scientific Vitrobot™ Mark IV System. Two grids were prepared for each spike-Fab complex. EPU Atlas Screening was used to collect atlas images of all 24 grids, and the 12 best grids (one from each duplicate pair) were selected for data acquisition.

Grid	Quantifoil R1.2/1.3
Camera	Selectris X Energy Filter and Falcon 4 Detector
Slit width (eV)	10
Nominal magnification	130,000x
Pixel size (Å)	0.929
Dose rate (e-/pix/sec)	5.3
Exposure time (sec)	8.32
Total dose (e-/Å^2)	48
Fractionation	EER
Autofocus	After centering
Hole centering	AFIS (6 µm image shift)
Number of images	12 x 1000
Throughput	~250/hour

Table 1. Cryo-EM data acquisition parameters.

The addition of binding partners introduces additional variables so it is valuable to screen grids before committing to data collection. EPU Multigrid can be used for screening by limiting the number of recorded movies using the "Max Exposures" option. To gauge the suitability of our twelve complexes for structural determination, we used EPU Multigrid on a Glacios Cryo-TEM to collect 50 movies per spike-Fab complex. These small datasets were preprocessed in cryoSPARC Live Software (Structura Biotechnology)[5]; particles were picked using a blob picker and 2D classified. All samples resulted in ~10,000 picked particles, and 2D classification displayed promising 2D class averages for all samples.

The twelve screened grids were then subjected to unattended EPU Multigrid data collection using a Thermo Scientific Krios™ G4 Cryo-TEM equipped with an E-CFEG, a Thermo Scientific Selectris™ X Energy Filter, and a Falcon 4 Detector operated in Electron-Event Representation (EER) mode. In a single, 48h-long EPU session, we set EPU Multigrid to collect 1,000 movies per grid, achieving a speed of 250 movies per hour. Data acquisition parameters are summarized in Table 1.

Sub-3-angstrom reconstructions using the Krios G4 Cryo-TEM

Data processing was performed using the cryoSPARC Software[5]. After patch-motion and CTF correction, particles were picked using a blob picker, extracted at 4x binning and subjected to 2D classification. Following 2D classification, particles belonging to class averages that displayed high-resolution detail were selected for ab-initio reconstruction into four classes. Tuned ab-initio parameters would generally split the data into two junk classes, one class with a closed spike (with no Fabs bound) and one with the full complex. Particles belonging to the whole complex class were re-extracted at 1.(3)x binning and subjected to non-uniform refinement with optimization of per-particle defocus and per-group CTF parameters[6]. All 12 spike-Fab complexes were resolved at resolutions better than 3 Å (see Table 2). Data processing took ~12 hours per dataset using a quad-GPU workstation.

Due to conformational dynamics relative to the rest of the spike trimer, the spike RBD-Fab regions were resolved to lower resolution. Further data processing was done to improve the local resolution at the epitope interface. For each complex, a cryoSPARC local refinement (BETA) was performed using a custom mask encompassing one RBD with the bound Fab. Despite the relatively small mass inside the local mask (~70 kDa), local refinement markedly improved local resolution, with all twelve epitope regions resolved to between 3.1 and 4.2 Å resolution (see Table 2).

Spike-Fab complex	Global resolution (Å)	Local resolution (Å)
Fab 1	2.8	**3.7**
Fab 2	2.7	**4.0**
Fab 3	2.9	**3.7**
Fab 4	2.9	**3.7**
Fab 5	2.8	**4.2**
Fab 6	2.5	**3.7**
Fab 7	2.9	**3.4**
Fab 8	2.4	**3.1**
Fab 9	2.8	**3.9**
Fab 10	2.6	**3.4**
Fab 11	2.5	**3.4**
Fab 12	2.9	**3.4**

Table 2. Global and local resolutions achieved for each spike-Fab complex.

The Fabs in this study were derived from pre-clinical development stage antibodies that are characterized by features such as neutralization of SARS-CoV-2 and variant pseudoviruses. To maintain confidentiality, detailed epitope classification of RBD-Fab interfaces is not described here. Instead, to highlight the resolutions achieved for the 12 spike-Fab complexes, we display densities from the spike S2 region and RBD, which represent global and local resolutions, respectively (Figure 3).

Conclusions

The combination of faster data acquisition schemes and faster cameras created the headspace to collect multiple cryo-EM datasets per day[7]. Data acquisition with EPU Multigrid allows

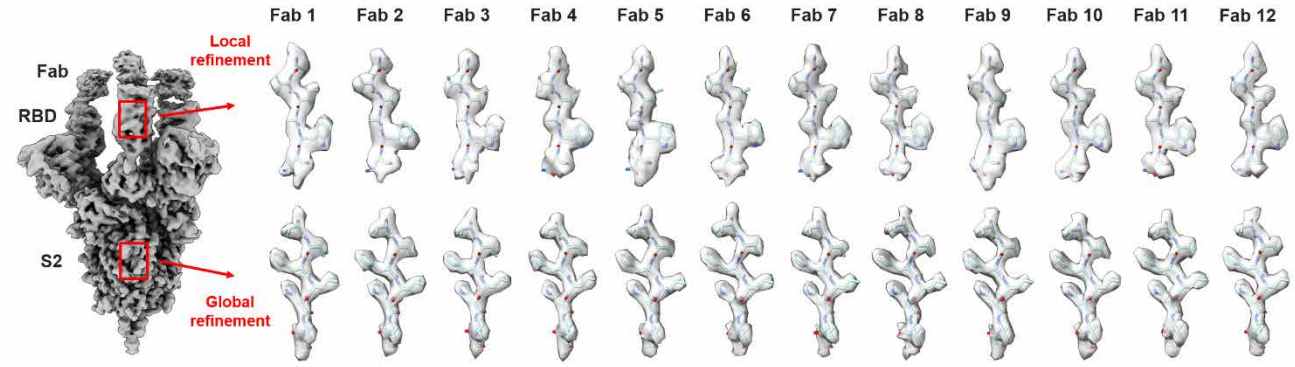

Figure 3. Representative S2 and RBD densities for 12 spike-fab complexes presented in this study. The S2 region is typically the best-resolved part of the spike; therefore, the S2 densities represent global resolution. In contrast, the RBD-Fab region is flexible and typically poorly resolved. In this study, local refinement of the RBD-Fab region was performed to improve the local resolution of the epitope. Therefore, RBD density is representative of local resolution achieved in the area adjacent to the epitope. The spike-Fab map shown in this figure is only to demonstrate the area from which density snippets were made, it does not correspond to any maps generated in this study.

users to collect data across multiple grids automatically. Here, we show that EPU Multigrid can be useful for screening and data collection, with the user deciding the desired number of movies per grid.

This workflow enabled us to obtain 12 sub-3-angstrom structures of the SARS-CoV-2 spike protein in complex with RBD-binding Fabs, and to determine their epitopes. Despite the relatively small size of each dataset and conservative nominal magnification used, our reconstructions are well resolved at the epitope-paratope interface. We attribute this achievement to the data's high quality, promoted by sample optimization and screening, as well as the assistance of the Selectris X Energy Filter and E-CFEG.

Our results show the significant advances that have been made in the speed, quality, and automation of cryo-EM data collection. We believe that cryo-EM's high-resolution revolution will soon be followed by a high-throughput revolution, which will improve existing applications through increased efficiency and reduced cost per dataset. It will also extend the range of cryo-EM applications to include fragment-based drug discovery[7] and epitope mapping of large antibody panels.

In summary, cryo-EM is now poised to emulate the success of macromolecular crystallography thanks to faster data collection and EPU Multigrid.

Acknowledgments

This work was partially funded by the Corona Accelerated R&D in Europe (CARE) project.The CARE project has received funding from the Innovative Medicines Initiative 2 Joint Undertaking (JU) under grant agreement No 101005077. The JU receives support from the European Union's Horizon 2020 Research and Innovation Programme, the European Federation of Pharmaceutical Industries and Associations, the Bill & Melinda Gates Foundation, the Global Health Drug Discovery Institute, and the University of Dundee. The content of this publication only reflects the author's view and the JU is not responsible for any use that may be made of the information it contains.

Antibody discovery was performed at Takeda Pharmaceuticals.

References

1. C. O. Barnes et al., *SARS-CoV-2 neutralizing antibody structures inform therapeutic strategies*, **Nature**, vol. 588, no. 7839, pp. 682–687, Dec. 2020, doi: 10.1038/s41586-020-2852-1.
2. J. Hansen et al., *Studies in humanized mice and convalescent humans yield a SARS-CoV-2 antibody cocktail*, **Science** (New York, N.Y.), vol. 369, no. 6506, pp. 1010–1014, Aug. 2020, doi: 10.1126/science.abd0827.
3. H. Ching-Lin et al., *Structure-based design of prefusion-stabilized SARS-CoV-2 spikes*, Science, vol. 369, no. 6510, pp. 1501–1505, Sep. 2020, doi: 10.1126/science.abd0826.
4. C. Yongfei et al., *Distinct conformational states of SARS-CoV-2 spike protein*, **Science**, vol. 369, no. 6511, pp. 1586–1592, Sep. 2020, doi: 10.1126/science.abd4251.
5. A. Punjani, J. L. Rubinstein, D. J. Fleet, and M. A. Brubaker, *cryoSPARC: algorithms for rapid unsupervised cryo-EM structure determination*, **Nature Methods**, vol. 14, no. 3, pp. 290–296, 2017.
6. A. Punjani, H. Zhang, and D. J. Fleet, *Non-uniform refinement: adaptive regularization improves single-particle cryo-EM reconstruction*, **Nature Methods**, vol. 17, no. 12, pp. 1214–1221, 2020, doi: 10.1038/s41592-020-00990-8.
7. M. Saur et al., "*Fragment-based drug discovery using cryo-EM*," **Drug Discovery Today**, vol. 25, no. 3, pp. 485–490, 2020, doi: https://doi.org/10.1016/j.drudis.2019.12.006.